Single-Molecule Behavior of Monomeric and Heteromeric Kinesins†

Daniel W. Pierce,*,‡,§ Nora Hom-Booher,‡ Anthony J. Otsuka,|| and Ronald D. Vale‡

Howard Hughes Medical Institute and Department of Cellular and Molecular Pharmacology, University of California, San Francisco, 513 Parnassus Avenue, San Francisco, California 94143, and Department of Biological Sciences, Illinois State University, Normal, IL 61761

Received December 21, 1998; Revised Manuscript Received February 25, 1999

ABSTRACT: Conventional kinesin is capable of long-range, processive movement along microtubules, a property that has been assumed to be important for its role in membrane transport. Here we have investigated whether the *Caenorhabditis elegans* monomeric kinesin unc104 and the sea urchin heteromeric kinesin KRP85/95, two other members of the kinesin superfamily that function in membrane transport, are also processive. Both motors were fused to green fluorescent protein, and the fusion proteins were tested for processive ability using a single-molecule fluorescence imaging microscope. Neither unc104-GFP nor KRP85/95-GFP exhibited processive movement (detection limit ∼40 nm), although both motors were functional in multiple motor microtubule gliding assays ($v = 1760 \pm 540$ and 202 ± 37 nm/s, respectively). Moreover, the ATP turnover rates (5.5 and 3.1 ATPs per motor domain per second, respectively) are too low to give rise to the observed microtubule gliding velocities, if only a single motor were driving transport with an 8 nm step per ATPase cycle. Instead, the results suggest that these motors have low duty cycles and that high processivity may not be required for efficient vesicle transport. Conventional kinesin's unusual processivity may be required for efficient transport of protein complexes that cannot carry multiple motors.

Kinesins are motor proteins that move along microtubules (MTs).[1] The kinesin superfamily is currently comprised of nearly 100 proteins grouped in 8 distinct subfamilies (*1*, *2*) that function in organelle transport, in mitotic and meiotic spindle assembly and function, and in maintenance and remodeling of the interphase structure of the cytoskeleton. All kinesins share an approximately 320 amino acid (aa) globular domain that is conserved at 30−40% identity throughout the superfamily and contains the ATP and MT binding sites. Outside of this motor domain, kinesins are quite divergent, and subfamily-specific structures formed by the remainder of the sequence mediate multimerization and cargo binding.

The best studied member of the kinesin superfamily is conventional kinesin, a vesicle transport motor. Conventional kinesin is a heterotetrameric enzyme with two identical heavy chains and two identical light chains (*3*, *4*). The ∼110 kDa heavy chains contain the kinesin motor domain at the N-terminus and are dimerized by an extended α-helical coiled-coil "stalk." Conventional kinesin has been shown to be a processive enzyme (*5*, *6*), capable of taking >100 steps of 8 nm length (*7*) along a MT before dissociating. The presence of two motor domains per molecule suggested that kinesin achieves processive motion by coordinating the activities of the motor domains so they interact with the MT in an alternating, hand-over-hand manner (*8*). Although this mechanism has not been directly demonstrated, it is consistent with available structural, motility, and kinetic data. Monomeric kinesin constructs are not processive (*9*−*13*), and the two motor domains of the dimer are kinetically distinct when interacting with a MT (*8*, *14*).

Despite the sequence similarity of the motor domains, other members of the kinesin superfamily have distinct chemomechanical properties from conventional kinesin. While the majority of kinesin motors moves toward the MT "+" end, the C-terminal subfamily (in which the motor domain is located at the carboxy terminus of the polypeptide) moves toward the "−" end (*15*, *16*). Measured velocities of movement of kinesins range from 40 nm/s for the Drosophila mitotic motor KRP130 (*17*) to 2500 nm/s for the conventional kinesin-related Nkin motor of Neurospora crassa (*18*).

Relatively little experimental information exists on the processivity of nonconventional kinesins. This property is of considerable interest, as it is expected to provide insight into the context in which a motor functions in vivo. Motors which function as part of a large group or array need not be processive, because other motors acting in parallel will maintain the connection to the filament when an individual motor dissociates (*19*). Motors that function as isolated

† Daniel W. Pierce was supported by a Jane Coffin Childs Foundation postdoctoral fellowship. The Howard Hughes Medical Institute provided support for this work.

* To whom correspondence should be addressed.

‡ University of California.

§ Present Address: Department of Chemistry and Biochemistry, 108 Gaines Hall, Montana State University, Bozeman, Montana 59717.

|| Illinois State University.

[1] Abbreviations: 2ME, 2-mercaptoethanol; aa, amino acid; ADP, adenosine diphosphate; AMP-PNP, 5′-adenylylimidodiphosphate; ATP, adenosine triphosphate; BSA, bovine serum albumin; DTT, dithiothreitol; EGTA, ethylene glycol bis-(aminoethyl ether)-*N*,*N*,*N*′,*N*′-tetraacetic acid; GFP, green fluorescent protein; GTP, guanosine triphosphate; Mops, 3-morpholinopropanesulfonic acid; MT, microtubule; NADH, β-nicotinamide adenine dinucleotide reduced form; NTA, nitrilotriacetic acid; PCR, polymerase chain reaction; pfu, plaque-forming units; Pipes, piperazine-*N*,*N*′-bis(2-ethanesulfonic acid); PMSF, phenylmethylsulfonyl fluoride; Tris, tris(hydroxymethyl)aminomethane.

10.1021/bi9830009 CCC: $18.00
Published on Web 04/09/1999

molecules or in small groups will become detached from the filament after one or a few steps unless they are processive, and therefore need to be processive if they are to drive long-distance transport events. Our laboratory has determined that a Ncd-GFP fusion protein is not detectably processive using the single-molecule fluorescence assay (*20*), a finding which has been corroborated by kinetic (*21*) and motility (*22*) measurements. Although these results showed that not all dimeric kinesins are processive, they were otherwise unsurprising because Ncd and Eg5 are thought to function as part of a large and stable structure (the spindle) (*23*) and have no obvious need for processive ability.

In this study, we wished to examine whether membrane-transporting kinesins other than conventional kinesin exhibit processive motion. Axonal transport vesicles are small (~100−400 nm in diameter), and electron micrographs of axoplasm (*24*, *25*) show one or a few crossbridges between vesicles and MTs. Because of these observations, it has been thought that transport of a vesicle may be driven by one or very few motor proteins. One important class of membrane transporters is the unc104/KIF1A family of monomeric kinesins. Murine KIF1A (*26*) and its *Caenorhabditis elegans* ortholog unc104 (*27*) have been shown to function in vivo in presynaptic vesicle transport (*28*, *29*). Monomeric kinesins lack the extended α-helical coiled-coil of conventional kinesin and are the only subfamily in which multimerization has not been experimentally found or strongly predicted from the amino acid sequence. Hirokawa and co-workers suggested that KIF1A is processive (*26*) on the basis of its qualitative behavior in MT gliding assays, presenting an interesting challenge to the "hand over hand" model for conventional kinesin movement.

Another important class of membrane transport kinesins is the kinesin II subfamily (also known as the heterotrimeric kinesins). This family is distinguished from other kinesins by the presence of two distinct, heterodimerized motor domains per molecule (*30*, *31*), both of which are closely related to the motor domain of conventional kinesin. Members of this family include sea urchin kinesin II, which localizes to cilia and ciliary basal bodies in motile embryos and is strongly implicated in intraflagellar transport (*32*−*34*), and the murine neuronal membrane transport motor KIF3A/B (*31*). KRP85/95 refers to dimers of the motor-containing subunits KRP85 and KRP95.

In this study, we determined the single-molecule behavior of GFP fusion proteins of the monomeric kinesin unc104 (*27*) and the heteromeric kinesin KRP85/95 (*35*) using a microscope capable of imaging the fluorescence of single GFP molecules at video rate (*10*, *36*, *37*). Although both unc104$_{653}$-GFP and KRP85/95-GFP were active motors in conventional gliding motility assays, neither motor exhibited long-distance processive motion in the single-molecule fluorescence assay. The measured ATPase rates for unc104$_{653}$-GFP and KRP85/95-GFP are too low for single motors to produce the observed MT gliding velocities. Overall, these results suggest that unc104$_{653}$-GFP and KRP85/95-GFP have a lower duty cycle than conventional kinesin, are not processive, and function more like myosin with individual motors making additive contributions to the MT gliding velocity. Our results suggest that processivity is not required for vesicle transport by kinesin motor proteins and raise the possibility that the processive ability of conventional kinesin is related to some other function in the cell.

EXPERIMENTAL PROCEDURES

Chemicals and Others

Except as noted, chemicals were obtained from Sigma. Restriction endonucleases and Taq polymerase were obtained from Life Technologies/Gibco or New England Biolabs. AMP−PNP was obtained from Boehringer Mannheim.

DNA Construct Generation

DNA manipulations were performed by standard methods, and all coding regions derived from PCR products were sequenced and found to be without errors in the final expression constructs.

(A) unc104$_{653}$-GFP. A DNA fragment encoding aa 1−653 of unc104 followed by a *Kpn*I restriction site (coding for the sequence Gly-Thr) was synthesized by polymerase chain reaction using the plasmid AO705 (*27*) as the template. The forward primer contained a *Nde*I site at the start codon. This PCR product was digested with *Nde*I and *Kpn*I. A pET17b-derived (Novagen) human kinesin-GFP expression plasmid (*38*) containing aa 1−560 of human ubiquitous conventional kinesin followed by a *Kpn*I restriction site (also coding for a Gly-Thr dipeptide), GFP, and a 6×His purification tag was digested with *Kpn*1 and *Xho*I and the fragment coding for GFP-6×His isolated. This same plasmid was then digested with *Nde*I and *Xho*I, the vector fragment isolated, and the unc104 and GFP fragments co-ligated with the vector fragment to give the plasmid unc104$_{653}$-GFP. In this construct, the GFP is C-terminal to the unc104 motor domain and is followed by a 6×His tag. In this and all other constructs described in this work, the S65T variant of GFP (*39*) was employed.

(B) KRP85-GFP and KRP95-GFP. The GFP portion of the KRP-GFP fusion constructs was generated by PCR. The forward primer contained a *Spe*I site upstream of the first six codons of GFP, and the reverse primer contained the last six codons of GFP followed by a 6×His sequence, a stop codon, and a *Xho*I site. The S65T mutant of GFP was used as a template to generate a PCR product, which was then digested with *Spe*I and *Xho*I and used for the three-way ligations described below.

85-pRSET and 95-pRSET plasmids (gift of Jon Scholey) were used as templates for PCR. The forward primers had a *Nde*I site at the start codon followed by codons 2−5 of either KRP85 or KRP95. The reverse primers contained the last six codons of either KRP85 or KRP95 followed by a *Spe*I site. The PCR products were digested with *Nde*I and *Spe*I and used for three-way ligations with the above *Spe*I-*Xho*I GFP fragment into the *Nde*I and *Xho*I sites of pET17b. The resulting constructs, pKRP85.7.GFP and pKRP95.7.GFP, have a Thr-Ser linker between the KRP and GFP.

The KRP-GFP fusion constructs were mutagenized using QuikChange (Stratagene) in order to subclone these fusions into a Baculovirus expression vector. Mutagenic oligos in the forward and reverse direction were designed to accomplish the two changes for each construct. The initation sequence upstream of the start codon was changed from ATCAT to ATAAT to optimize the expression levels in baculovirus, and the six-base sequence upstream of the initiation site was changed to a *Sma*I site for KRP85-GFP and a *Bam*HI site for KRP95-GFP. Mutant plasmids were

sequenced and digested with either *Sma*I or *Bam*HI and with *Xho*I. The resulting 2.9 kb fragments were ligated into pFastBac1 (Life Technologies/Gibco) at either the *Eco*RI site (filled in) or the *Bam*HI site and the *Sal*I site.

The resulting FastBac donor plasmids were transformed into DH10Bac (Life Technologies/Gibco) to generate recombinant bacmids, which were purified and transfected into sf9 cells.

Protein Expression and Purification

The procedures for bacterial expression of kinesin-GFP and unc104$_{653}$-GFP have been described (*38*). KRP85-GFP and KRP95-GFP were expressed in insect sf9 cells using the baculovirus expression system (Life Technologies/Gibco). Recombinant virus was generated according to the Bac-to-Bac baculovirus expression protocols (Life Technologies/Gibco). The time course of protein expression using the two recombinant viruses was assessed in 1 mL trials in a six-well tissue culture plate (1 mL in each 35 mm well) and found to peak at approximately 72 h post-inoculation. For large-scale expression, 250 mL cultures were infected with 3 mL of viral stock with a titer of 1.7×10^6 pfu to give a multiplicity of infection of approximately 0.15. For coexpression of KRP85-GFP and KRP95-GFP, the multiplicity of infection was 0.5 for each virus. Although this multiplicity does not ensure that all cells are infected with both viruses at the outset, it was difficult to obtain higher titer virus stocks, and most cells will become infected with both viruses during the 72 h incubation period.

Cells were harvested by centrifugation in a clinical centrifuge and cell pellets resuspended in lysis buffer (*38*) to a volume of 2.5 mL/g of cells, frozen between slabs of dry ice, and stored at −80°. For protein purification, frozen cell pellets were thawed and lysed on ice by the addition of 1% NP-40 (Boehringer) in the presence of 4 mM Pefablock (AEBSF, Boehringer), 0.5 mM ATP, 20 mM imidazole-Cl pH 8.0, 10 mM 2-mercaptoethanol (2ME), and >10 μM aprotinin and leupeptin. Lysis was verified by visualizing cells with Trypan Blue. The lysate was centrifuged for 30 min at 18 500 rpm in an SS-34 rotor at 4°. Nickel-NTA chromatography was performed as described (*38*) except that 0.25 mL of equilibrated resin slurry was added per liter of cell culture and 0.25 mL fractions were collected. Peak fractions (identified by faint green color and intense fluorescence when viewed through an appropriate filter set) were pooled, made 10% w/v in sucrose, and frozen and stored in liquid N_2.

Microtubule Affinity Purification

(A) unc104$_{653}$-GFP. Bovine brain tubulin was prepared by cycles of polymerization and depolymerization followed by phosphocellulose chromatography (*40*) and stored at −80°. Aliquots were thawed rapidly and aggregates removed by centrifugation at 100 000 rpm for 15 min at 4° in a TLA 120.1 rotor (Beckman). After addition of 0.5 mM GTP and 20 μM taxol (Sigma), samples were incubated at 37° for 30 min. MTs were sedimented for 10 min at 80 000 rpm and 25° in the TLA120.1 rotor through a cushion consisting of BRB80 buffer (80 mM K^+Pipes pH 6.8, 1 mM $MgCl_2$, and 1 mM EGTA) containing 20 μM taxol and 60% glycerol. The MT pellet was resuspended in $^1/_5$ of the original aliquot volume of BRB80 buffer containing 20 μM taxol. Motor protein column fractions were diluted 1:1 with BRB12 buffer (equivalent to BRB80 except that the Pipes concentration is 12 mM). Taxol (20 μM), 0.5 units/mL apyrase (Sigma), and MTs (4 mol of tubulin dimer/mol of motor) were added to the motor fractions and the samples incubated at room temperature for 10 min. MTs and associated motors were sedimented through a 60% glycerol cushion as described above. The pellets were washed with BRB80 buffer and resuspended in $^1/_4$ of the original motor aliquot volume of release buffer (BRB80 containing 5 mM MgATP, 200 mM KCl, and 20 μM taxol). After 5 min at room temperature, samples were centrifuged for 5 min at 80 000 rpm in a TLA120.l rotor to pellet the MTs. Supernatants containing the purified motors were either used immediately in experiments or made 10% in sucrose and frozen and stored in liquid N_2.

(B) KRP85/95-GFP. A Pharmacia NAP-5 desalting column was equilibrated with 4 column volumes of BRB80 containing 20 mg/mL bovine serum albumin (BSA) and allowed to stand for 30 min at room temperature. At 4°, the column was washed with 2 volumes of BRB80 containing 5 mg/mL BSA, 1 mM dithiothreitol (DTT), and 25 μM ATP. Nickel-NTA-purified KRP85/95-GFP (0.6 mL) was loaded, and 0.2 mL fractions were collected. The 5 peak fractions were identified by GFP fluorescence, pooled, and made 20 μM in taxol and 1 mM in AMP−PNP. A 4:1 molar excess of MTs (prepared as above) was added and the sample incubated for 15 min at room temperature. The remainder of the protocol was identical to that given for the unc104$_{653}$-GFP above.

Expression of Kinesin-GFP, unc104$_{653}$-GFP, and KRP85/95-GFP by in Vitro Translation and Axoneme Affinity Purification

In vitro translation was performed in rabbit reticulocyte lysate using the Promega T7 TnT coupled transcription and translation system according to the manufacturer's instructions. Translation mixtures (100 μL) were then microcentrifuged at 13000*g* for 10 min at 4°. Motor-GFP concentrations of the supernatants were determined by measuring the GFP fluorescence intensity of a 1:100 dilution of the translation mixture in BRB80. The supernatants were made 5 mM in Mg^{2+}AMP−PNP, and 2.5 μL of a 1.1 mg/mL solution of salt washed sea urchin sperm flagellar axonemes (*38*) was added. Samples were rotated at 4° for 30 min and then centrifuged for 5 min at 13000*g* and 4°. The axoneme pellets were first washed with and then resuspended in 50 μL of BRB12 supplemented with 50 mM KCl, 1 mM DTT, and 1 mg/mL BSA. After centrifugation at 13000*g* for 5 min at 4°, the axonemes were resuspended in 1.25 μL of BRB12 supplemented with 25 mM KCl, 1 mM DTT, 25 μM ATP, and 30 mg/mL BSA. This solution was used in place of the motor dilution in the single-molecule fluorescence assay protocol (*38*).

Immunoprecipitation of KRP85-GFP, KRP95-GFP, and KRP85/95-GFP Heterodimers

The KRP85-GFP and KRP95-GFP samples were purified by nickel affinity chromatography and stored in elution buffer. The KRP85/95-GFP sample was MT affinity-purified

and stored in release buffer. To make the buffers equivalent for all samples, we diluted the KRP85-GFP and KRP95-GFP samples 1:1 with release buffer, and the KRP85/95-GFP sample 1:1 with nickel elution buffer (*38*). All samples were then further diluted 2:1 with 7.5 mg/mL BSA in water. Mouse monoclonal antibodies K2.4 (*30*) or K2.5 (gift of J. Scholey) (1.5 μL) were added to 135 μL of the diluted motor samples. After a 40 min incubation on ice, samples were diluted 1:1 with RIPA (25 mM Tris−HCl pH 7.5, 50 mM NaCl, 0.5% NP-40, 0.1% sodium deoxycholate (Sigma), 1 mM phenylmethylsulfonyl fluoride (PMSF, Sigma), and 10 μM aprotinin). After an additional 30 min on ice, 5 μL of protein G beads that had been washed 3× with 20 volumes of RIPA was added. Samples were rotated at 4° for 40 min and the beads pelleted and washed 3× in 0.5 mL of RIPA. Samples were transferred to new microfuge tubes and washed with 0.5 mL of 50 mM Tris−HCl pH 7.5, and proteins were eluted from the beads by boiling for 5 min in a 6× SDS sample buffer.

Sucrose Density Gradient Centrifugation

Sucrose gradients (2.0 mL, 12−24%) in BRB80 supplemented with 1 mM DTT, and 50 μg/mL of pepstatin, aprotinin, and leupeptin were poured on ice in 4 steps and allowed to diffuse at 4° overnight. Motor proteins (KRP85/95-GFP ATP release, kinesin-GFP, and unc104$_{653}$-GFP) were diluted at least 10-fold with 25 mM K^+Pipes pH 6.8, 1 mM EGTA, 1 mM DTT, 300 mM NaCl, 50 μg/mL pepstatin, aprotinin, leupeptin, and 10% sucrose. Samples (50 μL) were layered on top of the gradients and the gradients centrifuged in a Beckman TLS-55 rotor at 55 000 rpm for 5.5 hours at 4°. Fractions (205 μL) were collected from the bottom of the gradients using a glass capillary. GFP fluorescence was quantitated in each fraction and the peak fraction number determined by fitting the fluorescence profile to a Gaussian. Standard proteins were apoferritin ($S = 17.6$), catalase ($S = 11.3$), aldolase ($S = 7.35$), BSA ($S = 4.31$), and ovalbumin ($S = 3.6$). Peak fractions of standards were determined by densitometry of Coomassie-stained SDS−PAGE gels and Gaussian fitting. Sedimentation coefficients were determined from a linear regression of the fraction number versus the S value.

Gel Filtration Analysis

Due to unacceptable nonspecific adsorption of motor proteins to the gel filtration resin at low ionic strength, columns were run at 4° in a buffer consisting of 50 mM K^+Mops pH 7.0, 200 mM NaCl, 1 mM $MgCl_2$, 1 mM DTT, 1 mM EGTA, and 0.1 mM ATP. Samples (50 μL) were injected onto a Superose 6 gel filtration column (Pharmacia). Elution volumes were determined by absorbance at 280 nm or by fluorescence. The same set of standards was employed as for the density gradients except that lysozyme was subsituted for ovalbumin, with $D_{20,w} = 3.61 \times 10^{-7}$, 4.11×10^{-7}, 4.46×10^{-7}, 6.05×10^{-7}, and 1.20×10^{-6} cm^2/s, respectively. Motor protein $D_{20,w}$ values were determined from a linear regression of $\log(D_{20,w})$ versus elution volume.

MT Gliding Assays

(A) Perfusion Chambers (Flow Cells). Cover slips were washed with 25% HNO_3 for 10 min, rinsed twice with deionized water, washed with 2 M NaOH for 10 min, washed 6× with deionized water, and air-dried before use. Flow cells were constructed using double-sided tape to space the cover slip from the slide.

(B) Assays. Dry flow cells (3−5 μL volume) were filled with an 0.8 mg/mL solution of an affinity-purified rabbit polyclonal anti-GFP antibody and allowed to stand for 5 min. Chambers were washed 2× with 50 μL of BRB80, and a dilution of the motor preparation in BRB80 containing 0.5 mg/mL casein was introduced and allowed to bind for 5 min. The chamber was again washed 2× with 50 mL of BRB80 and approximately 10 μg/mL MTs introduced in 50 μL of BRB80 buffer containing 2 mg/mL casein, 1 mM ATP, 20 μM taxol, and a coupled enzyme oxygen scavenger system consisting of glucose oxidase, glucose, catalase, and 2ME (*38*, *41*). MT movement was recorded onto sVHS videotape using a Zeiss Axioplan microscope equipped with differential interference contrast optics. MT velocities were scored using a computer equipped with a video overlay board with start and end points input via a screen-reading cursor.

ATPase Assays

ATPase assays were performed using the NADH-coupled enzyme method (*42*, *43*) in BRB12 buffer supplemented with 1 mM dithiothreitol. MTs were prepared as described for MT affinity purification above, except that they were resuspended in BRB12 buffer. ATP, phospho(enol)pyruvate, NADH, lactate dehydrogenase, and pyruvate kinase were combined with 0−30 μM MTs, and the reaction was started by the addition of 100−250 nM motor protein. Motor concentrations were determined by measuring the fluorescence intensity of dilutions of motor-GFP or purified GFP S65T in BRB80 supplemented with 0.5 mg/mL BSA (to prevent loss of protein by adsorption to the walls of the cuvette). The concentration of the purified GFP S65T was calculated from the absorbance at 488 ($\epsilon = 39\,200$ M^{-1} cm^{-1} (*39*)). The change in absorbance at 340 nm was recorded and the linear phase fit to a straight line. Slopes were converted to units of ATP turnover per motor domain per second and the data fit to a hyperbola using Origin (MicroCal).

Single-Molecule Fluorescence Assays

Except for experiments in different buffers, the assay procedures have been described (*38*, *44*). Alternate buffers tested are noted in the discussion.

RESULTS

Expression of unc104$_{653}$-GFP and KRP85/95-GFP

We wished to express a truncated version of the 1584 aa unc104 protein that would have a high probability of incorporating all parts of the sequence that are important for motor function. To select an appropriate truncation point, we examined the sequences of unc104 and KIF1B with the assumption that the regions involved in motor function would be conserved between these proteins. Comparison of unc104 and KIF1A is less informative, since they are orthologues and are similar throughout the sequence. For unc104 and KIF1B, there is high sequence identity in the motor domains (e.g., aa 1−345 of unc104 is 73% identical to KIF1B). In

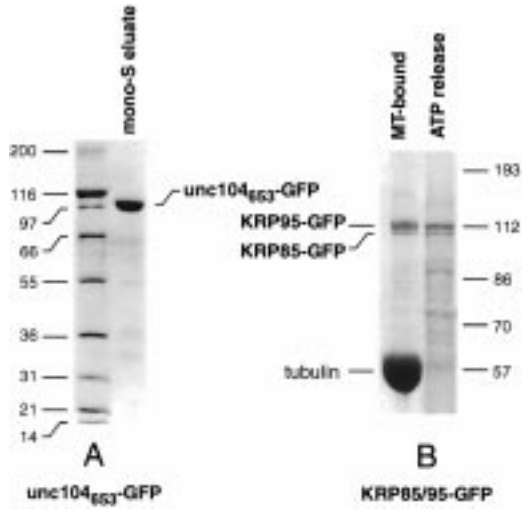

FIGURE 1: Summary of the purification of the unc104$_{653}$-GFP and KRP85/95-GFP. Panel A shows the peak fraction of the final mono-S column in the purification of unc104$_{653}$-GFP analyzed on a 4−12% gradient gel. Panel B shows the supernatant and pellet obtained in the MT release step of the KRP85/95-GFP purification. Note that the molar excess of KRP95-GFP is larger in the pellet (which contains motors that did not release from the MTs in the presence of ATP) than in the supernatant, where the mole ratio by Coomassie staining of KRP85-GFP to KRP95-GFP is 0.9.

an adjacent region from aa 345 to 635, unc104 is 50% identical to KIF1B. Beyond this region and extending toward the C-terminus, the amino acid identity falls abruptly to 20%. The PHD algorithm for secondary structure determination (*45*) indicates that unc104 contains a long α-helix extending from aa 619 to 652 which is terminated by three consecutive glycine residues. On the basis of the above considerations, we truncated unc104 at aa 653 and fused GFP (the S65T variant (*39*)) to the C-terminus. Figure 1A shows that unc104$_{653}$-GFP could be purifed to near homogeneity after expression in bacteria.

For sea urchin KRP85/95, we fused GFP C-terminal to the entire native sequences of both KRP85 and KRP95. Initial attempts at bacterial expression of KRP85-GFP and KRP95-GFP failed due to considerable proteolysis of the expressed proteins. To circumvent this problem, we expressed KRP85-GFP and KRP95-GFP using the baculovirus expression system. This method has the additional advantage of straightforward expression of heterodimers by co-infection of Sf9 insect cell cultures with the baculovirus vectors for each protein. Although yields are low compared to bacterial expression, there is very little proteolysis and the purification is relatively efficient after column chromatography and MT affinity purification (Figure 1B).

Oligomeric State of unc104$_{653}$-GFP and KRP85/95-GFP

We determined the oligomeric state of KRP85/95-GFP and unc104$_{653}$-GFP by a combination of classical hydrodynamic methods and measurement of the intensities of single-molecule fluorescence spots. We performed the latter measurements because we were unable to determine a diffusion constant for KRP85/95-GFP by gel filtration due to nonspecific adsorption to the column.

The sedimentation values of KRP85/95-GFP, unc104$_{653}$-GFP, and kinesin-GFP determined by sucrose density gradient centrifugation were 6.3 ± 0.4, 5.8 ± 0.3, and 6.9 ± 0.3 S, respectively. The diffusion constants ($D_{20,w}$) in cm^2/s of unc104$_{653}$-GFP and kinesin-GFP were determined by gel filtration chromatography and were $4.32 \pm 0.02 \times 10^{-7}$ and $3.12 \pm 0.03 \times 10^{-7}$, respectively. According to the Svedberg equation, the molecular mass of kinesin-GFP is 199 ± 7 kDa, in reasonable agreement with the predicted mass of 183 kDa for a dimer. The measured mass of unc104$_{653}$-GFP is 122 ± 7 kDa, near the predicted mass of 102 kDa for a monomer. The sedimentation coefficient of KRP85/95-GFP was intermediate between that of kinesin-GFP and unc104$_{653}$-GFP. The band obtained on the gradient was noticeably broader than that of either of the others, suggesting that the KRP85/95-GFP preparation contains a mixture of heterodimers and monomers.

The association state of KRP85/95-GFP was evaluated by comparing the fluorescence intensity of surface-bound motors adsorbed from dilute (0.5 nM) solutions (*36*). Measurements were performed on four constructs: kinesin-GFP, KRP85/95-GFP, unc104$_{653}$-GFP, and K339-GFP (a monomeric kinesin-GFP fusion protein containing the first 339 amino acids of human kinesin). The mean fluorescent spot intensities were 23213 ± 486 (N = 384), 17978 ± 514 (N = 312), 11791 ± 381 (N = 304), and 12616 ± 317 (N = 333), respectively (mean ± standard error of the mean). The values for kinesin-GFP, unc104$_{653}$-GFP, and K339-GFP are in the expected 2:1:1 ratio. The value for KRP85/95-GFP is intermediate, again suggesting that the preparation contains a mixture of heterodimers and monomers. A 67% mole fraction of heterodimers would lead to an average of 1.5 molecules of GFP per fluorescent spot.

Heterodimerization of KRP85/95-GFP

After MT affinity purification, the KRP85-GFP and KRP95-GFP polypeptides were present in nearly equal stoichiometry (Figure 1B), suggesting that they were present as a heterodimer. Densitometry of Coomassie-stained gels indicated a weight ratio of KRP85-GFP to KRP95-GFP of 0.82 for the MT releasate, corresponding to a mole ratio of 0.86. The mole ratio of the material that remained bound to the MTs in the presence of ATP was 0.55.

To prove that heterodimers were present, we performed immunoprecipitations using monoclonal antibodies specific for the two polypeptides (Figure 2). An antibody against KRP85 was able to precipitate KRP95-GFP from the MT releasate but was not able to precipitate KRP95-GFP in the absence of KRP85-GFP. Similarly, an antibody against KRP95 was able to precipitate KRP85-GFP, but only in the presence of KRP95-GFP. These results show that the MT releasate contains physically interacting KRP85-GFP and KRP95-GFP.

We estimated of the proportion of heterodimers versus homodimers and monomers in the MT releasate by comparing the efficiencies with which the antibodies precipitated each polypeptide (Figure 2). The immunoprecipitates obtained with either antibody contained comparable amounts of the two chains, demonstrating that the heterodimers constitute a significant fraction of the total protein. From the band intensities observed, this fraction is more similar to 100% than 20%, and we estimate that at least of 50% of the KRP85/95-GFP in the MT releasate is heterodimerized.

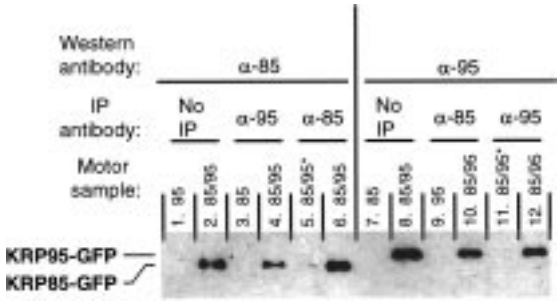

FIGURE 2: Immunoprecipitation of KRP85/95-GFP heterodimers. An α-KRP95 antibody (α-95) immunoprecipitates KRP85-GFP (lane 4), and correspondingly an α-KRP85 antibody (α-85) immunoprecipitates KRP95-GFP (lane 10), indicating that the two polypeptides are heterodimerized when coexpressed in sf9 cells. On the Western blot, α-85 does not cross-react with KRP95-GFP (lane 1) but detects KRP85-GFP (lane 2). Similarly, α-95 does not cross-react with KRP85-GFP (lane 7) but detects KRP95-GFP (lane 8). Both antibodies are also specific in the immunoprecipitations. In the absence of KRP95-GFP, α-95 does not precipitate KRP85-GFP (lane 3), and in the absence KRP85-GFP, α-85 does not precipitate KRP95-GFP (lane 9). When the same antibody is used for the immunoprecipitation and the Western blot (lanes 6 and 12), the bands are similar to those obtained when the two antibodies are used in sequence (lanes 4 and 10), showing that the sample contains a large proportion of heterodimers. The heterodimer fraction was estimated by using the same antibody for the immunoprecipitation and the Western blot, but loading 5-fold less immunoprecipitate (lanes 5 and 11). Since the bands were barely visible with this amount of epitope and much less intense than the bands in lanes 4 and 10, the sample must contain much more than 20% heterodimers. With allowance for the nonlinear response of the film, the proportion of heterodimers is at least 50%. Lanes marked with asterisks (*) contain $^1/_5$ of the amount of sample as the other lanes.

Gliding Motility and ATPase Activities of unc104$_{653}$-GFP and KRP85/95-GFP

Unc104$_{653}$-GFP and KRP85/95-GFP were both functional motors in multiple-motor MT gliding assays. The measured gliding velocities were 1760 ± 540 nm/s ($N = 33$) and 202 ± 37 nm/s ($N = 33$), respectively. The value for unc104$_{653}$-GFP is faster than that published for KIF1A (1200 nm/s) and much faster than the value (402 ± 87 nm/s, $N = 26$) obtained for kinesin-GFP in identical assays. Slower speeds and more efficient retention of MTs on the surface are observed for unc104$_{653}$-GFP at low ionic strength. The KRP85/95-GFP velocity is less than the value of 410 nm/s obtained for the native kinesin II heterotrimer purified from sea urchin eggs (*30*) but within the range of variation typically observed for assays performed on different constructs using different protocols.

ATPase assays were performed as a function of MT concentration and the data fit to a hyperbola (Figure 3). For KRP85/95-GFP, the basal hydrolysis rate was too slow to detect using this assay. The K_M for MT stimulation was 1.5 μM tubulin dimer, and the k_{cat} was 3.1 ATPs per motor domain per second. For unc104$_{653}$-GFP, the basal hydrolysis rate was significant and was 1.2 ATPs per motor domain per second. The K_M for MT stimulation was 32 μM tubulin dimer, and the k_{cat} was 5.5 per motor domain per second. Parallel assays performed on a dimeric kinesin construct (K560 (*42*) gave a K_M of 1.5 μM MTs and a k_{cat} of 28 ATPs per motor domain per second (data not shown).

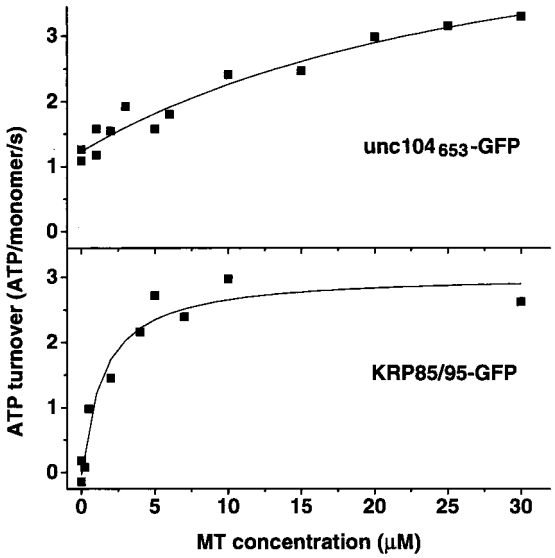

FIGURE 3: Microtubule-stimulated ATPase of unc104$_{653}$-GFP and KRP85/95-GFP. Hyperbolic fits to the data are indicated by solid lines. Fit parameters for unc104$_{653}$-GFP were the following: basal hydrolysis rate, 1.2 ATP head^{-1} s^{-1}; k_{cat}, 5.5 head^{-1} s^{-1}; and K_M-(MT), 32 μM. Fit parameters for KRP85/95-GFP were the following: k_{cat}, 3.1 head^{-1} s^{-1}; and K_M(MT), 1.5 μM. The basal hydrolysis rate for KRP85/95-GFP was too small to measure using this assay, and a basal rate parameter was not included in the fitting procedure.

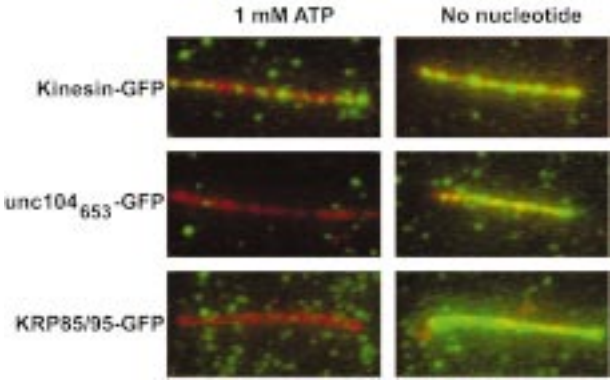

FIGURE 4: Images from single-molecule fluorescence motility assays. Fluorescence images of Cy5-labeled axonemes (pseudocolored red) were superimposed with GFP fluorescence images (pseudocolored green) of the same field. All images were obtained and processed identically. Single video frames recorded using a 4-frame rolling average are shown. The motor concentration is 0.5 nM. For kinesin-GFP in 1 mM ATP, axonemes are lightly decorated with moving spots, and the "+" end is labeled. In the absence of nucleotide, the axoneme is more heavily labeled along its length with immotile spots. For unc104$_{653}$-GFP and KRP85/95-GFP, there is no evident decoration of the axonemes at this or 40-fold higher motor concentrations in the presence of 1 mM ATP. However, the extent of axoneme labeling in the absence of nucleotide is similar to that observed for kinesin-GFP. Both the absence of observable movement and the absence of observable binding indicate that the interaction of these motors with axonemal MTs is transient in the presence of ATP.

Single-Molecule Motility of unc104$_{653}$-GFP and KRP85/95-GFP

Figure 4 shows a comparison of the behavior of 0.5 nM kinesin-GFP, unc104$_{653}$-GFP, and KRP85/95-GFP in the presence of ATP or apyrase (which hydrolyzes ATP to AMP and generates the nucleotide-free, rigor binding state of motor proteins). While kinesin-GFP molecules are readily observed moving on axonemal MTs in the presence of ATP, the same

conditions yield no detectable movement of unc104$_{653}$-GFP or KRP85/95-GFP during a minimum of 120 min of observation at motor concentrations ranging from 0.5 to 20 nM. In addition to the buffer composition employed in the kinesin-GFP assay (*38*), buffers containing 12 mM K^+Mops pH 7.0 instead of Pipes, and Pipes buffers supplemented with 75 or 150 mM NaCl or KCl, were also tested with similar results. Kinesin-GFP movement can be observed under these buffer conditions, although the association rate is reduced at higher salt concentrations (*10*). When a 1% mole fraction (0.2 nM) of kinesin-GFP was mixed with 20 nM unc104$_{653}$-GFP in the standard assay buffer, moving spots were observed at a rate of 5−10 events/min. This rules out the presence of an inhibitory factor in the unc104$_{653}$-GFP fraction and demonstrates that movement of a small mole fraction of active motors can be detected in the presence of a large background of inactive motors. If the unc104$_{653}$-GFP or KRP85/95-GFP constructs were as active and processive as kinesin-GFP, ~120000 events would have been detected during the 120 min of observation time.

To demonstrate that the proteins retain motor function under the conditions of the single-molecule fluoresence assay, we assessed the behavior of the constructs in the absence of ATP. ATP was omitted from the buffers, and 1 unit/mL apyrase added to destroy any nucleotide carried over with the diluted motor protein. Under these conditions (Figure 4), kinesin-GFP, unc104$_{653}$-GFP, and KRP85/95-GFP all decorated the axonemes with comparable efficiency. The motors are therefore capable of binding to axonemes in a nucleotide-dependent manner.

Single-Molecule Analysis Using In Vitro Translated Motors

We wished to express KRP85/95-GFP by an alternative method in order to ensure that motility assay results were not dependent on the expression system. Since the single-molecule fluorescence assay can be performed with extremely small amounts of material, we developed a new assay protocol for kinesin-GFP movement using in vitro translation. Transcription−translation reactions with the kinesin-GFP expression plasmid reproducibly yielded a translation mixture containing 10−20 nM GFP as determined by the measurement of GFP fluorescence. Western blotting of the translation mix using a mouse monoclonal anti-GFP antibody showed that full-length kinesin-GFP is the only band present that is not also found in negative controls in which the kinesin-GFP expression plasmid is omitted.

Although limited motility of kinesin-GFP can be observed by simply diluting the translation mixture in assay buffer, the translation mixture inhibits motility and must be diluted at least 20-fold. With an initial motor concentration of 10 nM, the maximum concentration that can be assayed is ~0.2 nM, which is near the limit at which movements are frequent enough to be readily detected. Hence, we sought a method for purifying very small amounts of motor proteins from in vitro translation reactions. The most successful method was to use sperm flagellar axoneme binding to purify and concentrate the motors (Figure 5). In assays using this motor fraction, axonemes were brightly labeled with moving motors, and we estimate that the motor concentration obtained was >20 nM. The run length determined from this

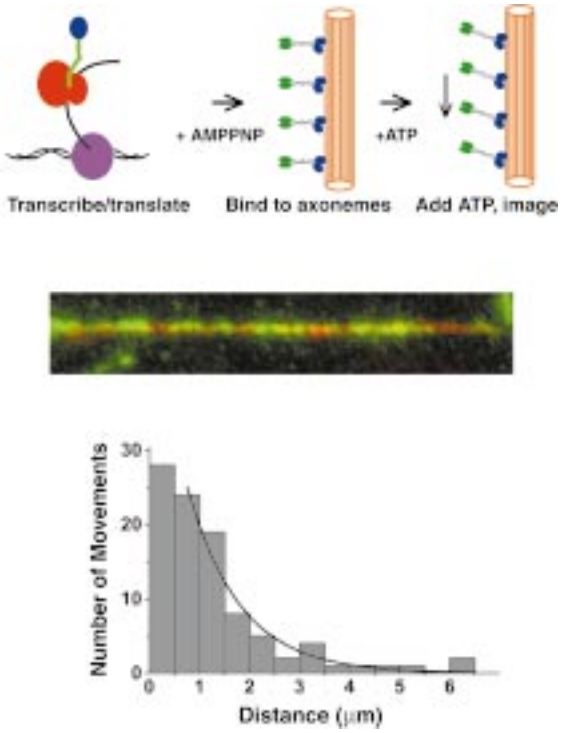

FIGURE 5: Assaying kinesin motors expressed by in vitro translation. The upper panel shows the assay protocol. The center panel shows an axoneme labeled with moving kinesin-GFP molecules and is intended to illustrate that expression is sufficient to detect numerous (thousands) events. The lower panel shows the distribution of travel distances obtained for kinesin-GFP expressed by in vitro translation. Events were scored after the sample was photobleached sufficiently that individual moving spots were clearly resolved from one another. The histogram was fit to a single-exponential decay (smooth curve), except for the first bin as it contains very short-lived events that may not be reliably detected. The decay constant is 1.05 μm but must be corrected for the effects of photobleaching (*37*). At the laser power employed, the corrected run length is 1.29 μm, which agrees with prior measurements (*6*, *37*).

in vitro translated kinesin-GFP was 1.29 μm, which is in agreement with prior measurements (*6*, *37*).

When KRP85-GFP and KRP95-GFP were translated individually, it was found that KRP95-GFP translates more efficiently, but 30 μg/mL KRP85-GFP and 10 μg/mL KRP95-GFP expression plasmid concentrations gave rise to nearly equal expression levels with motor concentrations of 10 ± 1 nM. Co-translation of KRP85-GFP and KRP95-GFP at the above template concentrations gave a final motor-GFP concentration of 9 nM, with approximately equal amounts of both polypeptides as evaluated by Western blotting using the GFP antibody. Previous investigations (*46*) have demonstrated heterodimerization of KRP85 and KRP95 by co-translation in in vitro translation reactions.

KRP85/95-GFP was purified in the same manner and with similar efficiency. However, as for KRP85/95-GFP expressed in sf9 cells, moving spots were not observed. This result further corroborates our conclusion that the KRP85/95-GFP construct described in this study is not detectably processive.

DISCUSSION

We have tested representatives of two kinesin subfamilies that have not been characterized with respect to processivity: the monomeric kinesins and kinesin II. Although both

families function in membrane transport, neither the monomeric kinesin unc104 nor the motor component of sea urchin kinesin II showed processive movement. Both motor preparations were active by other criteria, including the ability to glide MTs under multiple-motor conditions, the ability to bind to MTs in the presence of AMP−PNP or in the absence of nucleotide, and the ability to release from MTs in the presence of ATP or ADP.

The absence of processivity in the single-molecule assays is consistent with the results obtained in ATPase assays. Since kinesin is known to hydrolyze 1 ATP/8 nm step (*47*, *48*), one can predict the velocity of movement from the ATP turnover number. An ATP turnover number of 28 per motor domain per second, or 56 per molecule per second, should correspond to a movement velocity of $56 \times 8 = 448$ nm/s. This value is in reasonable agreement with the measured velocity of 402 nm/s. In contrast, the ATP turnover numbers determined for unc104$_{653}$-GFP and KRP85/95-GFP are too low to account for the measured velocities. To produce movement at 1760 nm/s while hydrolyzing 5.5 ATP/s, an unc104$_{653}$-GFP monomer would have to take 320 nm steps, while a KRP85/95-GFP dimer would have to take 33 nm steps to produce movement at 202 nm/s while hydrolyzing 6.2 ATP/s. While there is no reason to assume that the step size of a nonprocessive motor is 8 nm, these step sizes are not physically plausible. However, the ATPase and MT gliding data can be reconciled if the motors are working in a manner analogous to muscle myosin. Whereas a MT can be transported at the maximum velocity by a single conventional kinesin, individual myosin heads make additive contributions to the actin sliding velocity. The overall actin sliding velocity is therefore much higher than could be accounted for by the activity of a single myosin head. To work in this manner, a motor must have a low duty cycle, which is incompatible with processivity (*19*).

Single-molecule imaging of fluorescently labeled proteins has proved useful in the detection and quantification of processive movement by conventional kinesin (*38*). Three characteristics of this assay method render it, in our view, the method of choice for characterizing the processive ability of novel kinesins. First, the motor molecules are not adsorbed to the surface of a cover slip or a microsphere, avoiding the possibility of artifacts due to nonfunctional adsorption. Second, the fluorescence intensity gives a direct readout of the number of molecules participating in movement, so there is no ambiguity as to whether the experiment is measuring the properties of single molecules. Third, when GFP fusions are employed, there is no possibility of motor inactivation during chemical modification of the motor for surface attachment (e.g., biotinylation) or visualization (fluorescence labeling).

However, it is important to keep several characteristics of the assay method and the protein constructs in mind when interpreting these results. The assay has a limited spatial resolution. Although is it possible in principle to measure the position of the centroid of an object imaged in a light microscope with arbitrary accuracy, the signal-to-noise of single-molecule fluorescence images limits definition of the centroid to about half the dimension of a diffraction-limited source, or about 100 nm. Experience has shown that it is possible to detect and quantitate the processivity of a motor with a 1/e distance of 140 nm without great difficulty (*37*). For exponentially distributed travel distances, ~10% of all events will exceed the 100 nm threshold for detecting movement if the 1/e distance is ~40 nm. The processivity of a motor with a 1/e distance of less than 40 nm would not likely be detected in this assay, and would be more fruitfully investigated by kinetic or optical trapping approaches.

Although the constructs employed in this study are not highly processive, we cannot foreclose the possibility that the corresponding native motors have different properties. A failure to observe processive motion could be due to the nature of the constructs, the absence of regulatory cofactors in the in vitro assays, or some form of subtle denaturation that impairs processivity without abolishing the ATPase or MT binding activity. For example, in the case of unc104, it is possible that the C-terminal domain not present in unc104$_{653}$-GFP could somehow act to maintain an association with the MT when the motor domain dissociates. However, preliminary studies showed that an 800 aa unc104 construct also did not show processive motility. Alternatively, unc104-family motors may exist as larger complexes during active transport. In this regard, it is interesting that unc104-family motors have several segments of weakly predicted α-helical coiled-coil immediately C-terminal to the motor domain. It is possible that, when docked onto a membrane receptor or otherwise assembled into a larger complex, this coiled-coil forms and unc104 motor domains function similarly to those of dimeric conventional kinesin.

After this study was submitted, Okada and Hirokawa (*49*) reported that a chimeric protein containing aa 1−356 of KIF1A, followed by aa 330−351 of the murine conventional kinesin KIF5C, engaged in long distance movements along MTs as determined by a single-molecule fluorescence assay. Although KIF1A drives MT movement at 1200 nm/s in gliding assays, the observed single-molecule movements had an average velocity of 140 nm/s and included pauses and movements toward the presumed MT "−" end. This character of movement is more akin to a "biased diffusion" and is clearly distinct from the movement of conventional kinesin or of other processive enzymes such as polymerases, helicases, and ribosomes. The k_{cat} for the chimera was 20-fold larger than the value for unc104$_{653}$-GFP (110 vs 5.5 ATP s^{-1}), and the kinetics were consistent with a large (690 ATPs per interaction with a MT) chemical processivity. Okada and Hirokawa proposed that KIF1A is tethered to the MT by nonspecific electrostatic interactions between the negatively charged MT surface and a loop (L12) containing six lysine residues, which is uniquely conserved among the monomeric kinesin subfamily.

What could explain the differences between our observations for unc104$_{653}$-GFP and the KIF1A-KIF5C chimera? Unc104$_{653}$-GFP was functionally purified by MT affinity prior to performing ATPase or motility assays, so it is unlikely that the lower k_{cat} value and lack of movement are a consequence of inactive motors in the preparation. Okada and Hirokawa did not observe processive movement of nearly full-length KIF1A (*49*) in the single-molecule fluorescence assay, so it is possible that sequences C-terminal to the motor domain inhibit biased diffusional movement in vitro. The role of the conventional kinesin neck linker in the KIF1A-KIF5C chimera is also unclear. Furthermore, the sequences of the lysine loops in unc104 and KIF1A are distinct (the unc104 loop is shorter, has a lower net charge, and contains

a total of 5 lysines vs 6 in KIF1A). In summary, the differences in processivity and ATPase obtained here and by Okada and Hirokawa (*49*) are most reasonably attributed to differences in the constructs, and further work will be necessary to delineate which features are responsible for these distinct motor interactions with the microtubule.

For KRP85/95-GFP, the KRP85 and KRP95 chains were not truncated, and it is unlikely that the GFP is masking a functionally important site at the C-terminus. However, KRP85/95-GFP could exist in a folded, inhibited state as has been proposed for conventional kinesin (*50*, *51*). The predicted KRP85/95 coiled-coil stalk is interrupted by two glycines at positions 480/481 and 474/475 in the KRP85 and KRP95 sequences, respectively. Both sets of glycines are in positions d and e of the predicted coiled-coil, are likely apposed to each other in the structure, and could serve as a hinge region that allows the tail domain to fold against and inhibit the motor domains. In support of this idea, the addition of salt causes a transition in the *S* value of native kinesin II (*52*). However, we found that salt addition did not unmask the processive motion of KRP85/95-GFP. Inhibition of KRP85/95-GFP at low salt would have to be extremely efficient to frustrate detection of an intrinsically processive motor, as a 1% mole fraction of contaminating conventional kinesin-GFP can easily be detected in the presence of a high background of nonprocessive motors. Kinesin-GFP is truncated at aa 560 just prior to the hinge to prevent formation of a folded, inhibited state. Nevertheless, inhibition by this mechanism does not prevent detection of conventional kinesin's processivity, as we have been able to detect the very low-frequency movements of heterotetrameric conventional kinesin (full-length heavy chains plus light chains) (D. Friedman and R. Vale, unpublished observations).

Five of the approximately eight (*1*, *2*) subfamilies of the kinesins have now been tested for processive motion. We (*20*) and others (*21*, *22*) have reported that the Drosophila meiotic kinesin Ncd is not highly processive. By kinetic studies of ATPase activity, Crevel et al. also reported that the bimC-subfamily kinesin Eg5 is not processive. Therefore the conventional kinesin subfamily is thus far unique among all kinesin motors tested with regard to its high degree of processivity.

The absence of processivity by Eg5 and Ncd is not surprising since these may function as arrays in the mitotic/meiotic spindle. While it has been speculated that organelle transport requires highly processive motors, the evidence that axonal vesicles are transported a single crossbridge between the vesicle and the MT is not compelling and there are no direct in vivo measurements of the number of motors present on vesicles. The potential relevance of the biased diffusional movement of the KIF1A-KIF5C chimera (*49*) to vesicle transport in vivo is also unclear. A motor that diffuses rapidly along the MT during part of its enzymatic cycle would be compromised in its ability to exert a sustained force. Interestingly, some studies have indicated that motors may cluster in patches on the membrane surface (*53*), and this may serve as a mechanism enabling long-range transport. Recent experiments with single-headed, nonprocessive conventional kinesin constructs indicate that only 4−6 such motors are required to obtain reasonably continuous transport of a MT in gliding assays (*11*).

If processivity is not required of membrane transporters, why is conventional kinesin so highly processive? It is possible that kinesin's processivity is related to another function, for example, the transport of individual protein molecules or complexes that contain only one motor binding site. In this case, not only the number of motor binding sites is limited but also the diffusion constant of the cargo is very large compared to a vesicle and would rapidly separate a detached motor from the filament. The intriguing recent report (*54*) that conventional kinesin transports a small vimentin-containing particle and participates in the organization of the intermediate filament cytoskeleton may be an example of this type of process.

ACKNOWLEDGMENT

Jonathan Scholey and co-workers generously provided plasmids carrying the KRP85 and KRP95 sequences as well as the K2.4 and K2.5 antibodies.

REFERENCES

1. Vale, R. D., and Fletterick, R. J. (1997) *Annu. Rev. Cell Dev. Biol. 13*, 745−777.
2. Hirokawa, N. (1998) *Science 279*, 519−526.
3. Bloom, G. S., Wagner, M. C., Pfister, K. K., and Brady, S. T. (1988) *Biochemistry 27*, 3409−16.
4. Kuznetsov, S. A., Vaisberg, E. A., Shanina, N. A., Magretova, N. N., Chernyak, V. Y., and Gelfand, V. I. (1988) *EMBO J. 7*, 353−6.
5. Howard, J., Hudspeth, A. J., and Vale, R. D. (1989) *Nature 342*, 154−158.
6. Block, S. M., Goldstein, L. S., and Schnapp, B. J. (1990) *Nature 348*, 348−352.
7. Svoboda, K., Schmidt, C. F., Schnapp, B. J., and Block, S. M. (1993) *Nature 365*, 721−727.
8. Hackney, D. D. (1994) *Proc. Natl. Acad. Sci. U.S.A. 91*, 6865−6869.
9. Berliner, E., Young, E. C., Anderson, K., Mahtani, H., and Gelles, J. (1995) *Nature 373*, 718−721.
10. Vale, R. D., Funatsu, T., Pierce, D. W., Romberg, L., Harada, Y., and Yanagida, T. (1996) *Nature 380*, 451−453.
11. Hancock, W. O., and Howard, J. (1998) *J. Cell Biol. 140*, 1395−1405.
12. Ma, Y.-Z., and Taylor, E. W. (1997) *J. Biol. Chem. 272*, 717−723.
13. Jiang, W., and Hackney, D. D. (1997) *J. Biol. Chem. 272*, 5616−5621.
14. Ma, Y.-Z., and Taylor, E. W. (1997) *J. Biol. Chem. 272*, 724−730.
15. Walker, R. A., Salmon, E. D., and Endow, S. A. (1990) *Nature 347*, 780−782.
16. McDonald, H. B., Stewart, R. J., and Goldstein, L. S. (1990) *Cell 63*, 1159−1165.
17. Cole, D. G., Saxton, W. M., Sheehan, K. B., and Scholey, J. M. (1994) *J. Biol. Chem. 269*, 22913−22916.
18. Steinberg, G., and Schliwa, M. (1995) *Mol. Biol. Cell 6*, 1605−1618.
19. Howard, J. (1997) *Nature 389*, 561−571.
20. Case, R. B., Pierce, D. W., Hom-Booher, N., Hart, C. L., and Vale, R. D. (1997) *Cell 90*, 959−966.
21. Crevel, I. M., Lockhart, A., and Cross, R. A. (1997) *J. Mol. Biol. 273*, 160−170.
22. Stewart, R. J., Semerjian, J., and Schmidt, C. F. (1998) *Eur. Biophys. J. 27*, 353−360.
23. Endow, S. A., and Komma, D. J. (1997) *J. Cell Biol. 137*, 1321−1336.
24. Miller, R. H., and Lasek, R. J. (1985) *J. Cell Biol. 101*, 2181−2193.
25. Hirokawa, N., Pfister, K. K., Yorifuji, H., Wagner, M. C., Brady, S. T., and Bloom, G. S. (1989) *Cell 56*, 867−878.

26. Okada, Y., Yamazaki, H., Sekine-Aizawa, Y., and Hirokawa, N. (1995) *Cell 81*, 769−780.
27. Otsuka, A. J., Jeyaprakash, A., Garcia, A. J., Tang, L. Z., Fisk, G., Hartshorne, T., Franco, R., and Born, T. (1991) *Neuron 6*, 113−22.
28. Yonekawa, Y., Harada, A., Okada, Y., Funakoshi, T., Kanai, Y., Takei, Y., Terada, S., Noda, T., and Hirokawa, N. (1998) *J. Cell Biol. 141*, 431−441.
29. Hall, D. H., and Hedgecock, E. M. (1991) *Cell 65*, 837−847.
30. Cole, D. G., Chinn, S. W., Wedaman, K. P., Hall, K., Vuong, T., and Scholey, J. M. (1993) *Nature 366*, 268−270.
31. Yamazaki, H., Nakata, T., Okada, Y., and Hirokawa, N. (1995) *J. Cell Biol. 130* (6), 1387−1399.
32. Morris, R. L., and Scholey, J. M. (1997) *J. Cell Biol. 138*, 1009−1022.
33. Henson, J. H., Cole, D. G., Roesener, C. D., Capuano, S., Mendola, R. J., and Scholey, J. M. (1997) *Cell Motil. Cytoskeleton 38*, 29−37.
34. Cole, D. G., Diener, D. R., Himelblau, A. L., Beech, P. L., Fuster, J. C., and Rosenbaum, J. L. (1998) *J. Cell Biol. 141*, 993−1008.
35. Cole, D. G., Cande, W. Z., Baskin, R. J., Skoufias, D. A., Hogan, C. J., and Scholey, J. M. (1992) *J. Cell Sci*.
36. Pierce, D. W., Hom-Booher, N., and Vale, R. D. (1997) *Nature 388*, 338−338.
37. Romberg, L., Pierce, D. W., and Vale, R. D. (1998) *J. Cell Biol. 140*, 1407−1416.
38. Pierce, D. W., and Vale, R. D. (1998) *Methods Enzymol. 298* (Molecular Motors and the Cytoskeleton, Part B), 154−171.
39. Heim, R., Cubitt, A. B., and Tsien, R. Y. (1995) *Nature 373*, 663−664.
40. Williams, R. C. J., and Lee, J. C. (1982) *Methods Enzymol. 85*, 376−385.
41. Harada, Y., Sakurada, K., Aoki, T., Thomas, D. D., and Yanagida, T. (1990) *J. Mol. Biol. 216*, 49−68.
42. Woehlke, G., Ruby, A. K., Hart, C. L., Ly, B., Hom-Booher, N., and Vale, R. D. (1997) *Cell 90*, 207−216.
43. Huang, T. G., Suhan, J., and Hackney, D. D. (1994) *J. Biol. Chem. 269*, 16502−16507.
44. Pierce, D. W., and Vale, R. D. (1998) *Methods Cell Biol. 58* (GFP Biofluorescence: Imaging Gene Expression and Protein Dynamics in Living Cells), 49−73.
45. Rost, B., and Sander, C. (1993) *J. Mol. Biol. 232*, 584−599.
46. Rashid, D. J., Wedaman, K. P., and Scholey, J. M. (1995) *J. Mol. Biol. 252*, 157−162.
47. Hua, W., Young, E. C., Fleming, M. L., and Gelles, J. (1997) *Nature 388*, 390−393.
48. Schnitzer, M. J., and Block, S. M. (1997) *Nature 388*, 386−390.
49. Okada, Y., and Hirokawa, N. (1999) *Science 283*, 1152−1157.
50. Hackney, D. D., Levitt, J. D., and Suhan, J. (1992) *J. Biol. Chem. 267*, 8696−701.
51. Hackney, D. D. (1995) *Nature 377*, 448−450.
52. Wedaman, K. P., Meyer, D. W., Rashid, D. J., Cole, D. G., and Scholey, J. M. (1996) *J. Cell Biol. 132*, 371−380.
53. Leopold, P. L., McDowall, A. W., Pfister, K. K., Bloom, G. S., and Brady, S. T. (1992) *Cell Motil. Cytoskeleton 23*, 19−33.
54. Prahlad, V., Yoon, M., Moir, R. D., Vale, R. D., and Goldman, R. D. (1998) *J. Cell Biol. 143*, 159−170.

BI9830009